A New Robust Kalman Filter for SINS/DVL Integrated Navigation System

LI LUO, YONGGANG ZHANG, (Senior Member, IEEE), TAO FANG, AND NING LI
College of Automation, Harbin Engineering University, Harbin 150001, China
Corresponding author: Yonggang Zhang (zhangyg@hrbeu.edu.cn)

ABSTRACT A new robust strap-down inertial navigation system (SINS) and Doppler velocity log (DVL) integrated navigation algorithm are proposed in this paper with a focus on suppressing the process uncertainty and measurement outliers induced by severe manoeuvering. In the proposed algorithm, the one-step predicted probability density function is modeled as Student's t-distribution to deal with the heavy-tailed process noise, and hierarchical Gaussian state-space model for SINS/DVL integrated navigation algorithm is constructed. To detect and eliminate the measurement outliers, each measurement is marked by a binary indicator variable modeled as a beta-Bernoulli distribution. The variational Bayesian approach is used to jointly estimate state vector, auxiliary random variable, scale matrix, Bernoulli variable, and beta variable. The experimental results illustrate that the proposed algorithm has better robustness and navigation accuracy to deal with process uncertainty and measurement outliers than existing state-of-the-art algorithms.

INDEX TERMS Measurement outlier, process uncertainty, SINS/DVL integrated navigation system, variational Bayesian.

I. INTRODUCTION

Strap-down inertial navigation system (SINS) can continuously provide position, velocity, and attitude by the measurements of gyroscopes and accelerometers, however, its position and velocity errors are accumulated over time [1]–[3]. Doppler velocity log (DVL) can provide velocity by the principle of Doppler effect, but it can't provide attitude of the vehicle. SINS/DVL integrated navigation system combines the outputs of SINS and DVL, which can provide a long term accuracy position, velocity, and attitude information [4], [5]. For SINS/DVL integrated navigation system, the state-space model can easily be linearised. According to the linear model of SINS/DVL integrated navigation system, the navigation errors can be estimated by Kalman filter (KF) when the statistics of process noise and measurement noise are known as Gaussian distributions [6]. However, in the case of severe manoeuvering, such as turning and oscillating, the output error of the gyroscope may increase, and the inertial navigation error will increase with the output error of the gyroscope [7], [8]. Thus, the inertial navigation error will be introduced into the process model causing process uncertainty, and the heavy-tailed distribution process noise is

induced by the process uncertainty and gyroscope error [3]. Due to the complexity of underwater environment, such as gulf, ocean trench, and ocean current, the velocity provided by DVL may have outliers, which may also degrade the estimation accuracy of integrated navigation system.

To address the process uncertainty, a series of adaptive Kalman filters (AKFs), such as multiple model AKF (MMAKF) [9], [10] and Sage-Husa AKF (SHAKF) [4], [11] were proposed to estimate the statistic of the process noise. The MMAKF runs with multiple Kalman filters to address the process uncertainty, however, it suffers from a large amount of computation [12]. The SHAKF adopts the maximum posterior criterion to estimate the statistic of process noise, but it's easy to cause the divergence of the filter [13]. Thus, a type of robust Student's t based Kalman filters (RSTKF) is proposed [14]–[18]. In [16], Student's t-distribution is used to model the heavy-tailed process noise and measurement noise which may contain some valid information, but its performance will degrade when the measurement carries useless outliers. Aiming at reducing the impact of ouliers in measurement, a robust Kalman filter with outliers detection (ODKF) is proposed [19]. In ODKF, the measurement is assigned a binary indicator variable modelled by the beta-Bernoulli distribution to detect and eliminate the outliers, which has been successfully used to

address outliers [19]–[21], but the ODKF is applicable to the case where the process noise is Gaussian distribution and the statistic of process noise is accurately known. For SINS/DVL integrated navigation system with process uncertainty and measurement outlier, the performance will degrade, as will be shown by later simulations.

In order to suppress the process uncertainty and measurement outlier, a robust Kalman filter for SINS/DVL integrated navigation system is proposed in this paper. First, a new state-space model for SINS/DVL integrated navigation system is constructed. For process uncertainty, the one-step predicted probability density function (PDF) is modelled as a Student's t-distribution to deal with the heavy-tailed process noise. To detect the measurement outliers, the measurement likelihood PDF is involved in a binary indicator variable modelled by beta-Bernoulli hierarchical prior. Then, the navigation errors of SINS/DVL integration are estimated by the new robust Kalman filter, where the state vector, scale matrix, auxiliary random variable, Bernoulli variable, and beta variable are jointly estimated through variational Bayesian (VB) method. Finally, the position, velocity, and attitude can be corrected with the estimated navigation errors. Experiment results show that the proposed algorithm has better navigation performance to address the process uncertainty and measurement noise of SINS/DVL integrated navigation system than existing state-of-the-art algorithms.

This paper is organized as follows. In Section II, a linear state-space model for SINS/DVL integrated navigation system is modelled by the error propagation equations. Section III derives the proposed robust KF by using VB approach. Finally, experiment results are reported in Section IV, and conclusions are given in Section V.

II. STATE-SPACE MODEL FOR SINS/DVL INTEGRATED NAVIGATION SYSTEM

The process model for SINS/DVL integrated navigation system can be constructed by the position error equation, velocity error equation, and attitude error equation of SINS. Suppose that the calibration errors and installation errors of the accelerometers and gyroscopes have been compensated, the attitude error equation of SINS is given by [22], [23]

$$\dot{\boldsymbol{\varphi}} = \boldsymbol{\varphi} \times \boldsymbol{\omega}_{in}^n + \delta\boldsymbol{\omega}_{in}^n - \mathbf{C}_b^n \delta\boldsymbol{\omega}_{ib}^b \quad (1)$$

where i denotes inertial frame, e is the earth frame, n is the local level navigation frame (East-North-Up), and b denotes the body frame. $\boldsymbol{\varphi} = \begin{bmatrix} \varphi_E & \varphi_N & \varphi_U \end{bmatrix}^T$ denotes the misalignment angle vector of the navigation frame, and φ_E, φ_N, φ_U denote pitch, roll, and heading errors, respectively. $\boldsymbol{\omega}_{in}^n = \boldsymbol{\omega}_{ie}^n + \boldsymbol{\omega}_{en}^n$ is the angular rate of the navigation frame with respect to the inertial frame, and $\delta\boldsymbol{\omega}_{in}^n = \delta\boldsymbol{\omega}_{ie}^n + \delta\boldsymbol{\omega}_{en}^n$ denotes the corresponding calculated error of $\boldsymbol{\omega}_{in}^n$. $\boldsymbol{\omega}_{ie}^n$ is the earth rotation rate in the navigation frame, and $\delta\boldsymbol{\omega}_{ie}^n$ denotes the calculated error of $\boldsymbol{\omega}_{ie}^n$. $\boldsymbol{\omega}_{en}^n$ is the angular rate of the navigation frame with respect to the earth frame, and $\delta\boldsymbol{\omega}_{en}^n$ denotes the calculated error of $\boldsymbol{\omega}_{en}^n$. $\mathbf{C}_b^n(t)$ is the coordinate transformation matrix of the body frame with respect to the navigation frame,

and the gyroscope drift error $\delta\boldsymbol{\omega}_{ib}^b$ consists of constant drift $\boldsymbol{\varepsilon}^b$ and random drift $\boldsymbol{\eta}_g^b$.

The velocity error equation is written as [22], [23]

$$\delta\dot{\mathbf{v}}^n = \left(\mathbf{C}_b^n \mathbf{f}^b\right) \times \boldsymbol{\varphi} - (2\boldsymbol{\omega}_{ie}^n + \boldsymbol{\omega}_{en}^n) \times \delta\mathbf{v}^n$$
$$+ \mathbf{v}^n \times (2\delta\boldsymbol{\omega}_{ie}^n + \delta\boldsymbol{\omega}_{en}^n) + \mathbf{C}_b^n \delta\mathbf{f}^b + \delta\mathbf{g}^n \quad (2)$$

where $\mathbf{v}^n = \begin{bmatrix} v_E^n & v_N^n & v_U^n \end{bmatrix}$ and $\delta\mathbf{v}^n = \begin{bmatrix} \delta v_E^n & \delta v_N^n & \delta v_U^n \end{bmatrix}$ denote the ground velocity in the navigation frame and corresponding velocity error respectively. $\mathbf{f}^b$ and $\delta\mathbf{f}^b$ denote the specific force measured by the accelerometer and measurement error of accelerometer respectively, and the measurement error $\delta\mathbf{f}^b$ consists of accelerometer bias $\boldsymbol{\nabla}^b$ and random drift $\boldsymbol{\eta}_a^b$. $\delta\mathbf{g}^n$ is the gravity error.

The position error equations are given by [22], [23]

$$\delta\dot{L} = \frac{\delta v_N^n}{R_M + h} - \frac{v_N^n}{(R_M + h)^2}\delta h \quad (3)$$

$$\delta\dot{\lambda} = \frac{\sec L}{R_N + h}\delta v_E^n + \frac{v_E^n \sec L \tan L}{R_N + h}\delta L - \frac{v_E^n \sec L}{(R_N + h)^2}\delta h \quad (4)$$

$$\delta\dot{h} = \delta v_U^n \quad (5)$$

where L, λ, and h denote latitude, longitude and height of the vehicle, and the corresponding latitude error, longitude error, and height error are respectively denoted by δL, $\delta\lambda$ and δh. R_N is the curvature radius of the prime vertical circle, and R_M denotes the curvature radius of the meridian circle.

The velocity $\tilde{\mathbf{v}}_{dvl}^n$ provided by DVL can be written as

$$\tilde{\mathbf{v}}_{dvl}^n = [\mathbf{I}_{3\times3} - \boldsymbol{\varphi}\times]\mathbf{C}_b^n(1 - \boldsymbol{\alpha}\times)(1 + \delta c)\mathbf{v}^d$$
$$\approx \mathbf{v}^n + \mathbf{v}^n \times \boldsymbol{\varphi} + \mathbf{C}_b^n(\mathbf{v}^d\times)\boldsymbol{\alpha} + \mathbf{C}_b^n \mathbf{v}^d \delta c$$
$$= \mathbf{v}^n + \mathbf{v}^n \times \boldsymbol{\varphi} + \delta\mathbf{v}_{dvl}^n \quad (6)$$

where $\mathbf{v}^d$ is the velocity measured by DVL, $\boldsymbol{\alpha}$ is the installed error vector, δc denotes scale factor error.

In this paper, the SINS/DVL navigation system model used in surface navigation is established, which ignores the effect of altitude channel, and the corresponding process equation can be formulated as follow

$$\dot{\mathbf{x}}(t) = \mathbf{A}(t)\mathbf{x}(t) + \mathbf{B}(t)\mathbf{w}(t) \quad (7)$$

where $\mathbf{x}(t) = \begin{bmatrix} \boldsymbol{\varphi}^T & (\delta\mathbf{v})_{2,1}^T & \delta L & \delta\lambda & (\boldsymbol{\varepsilon}^b)^T & (\boldsymbol{\nabla}^b)^T \end{bmatrix}^T$ is the state vector, and $\mathbf{w}(t)$ is the process noise. $\mathbf{A}(t)$ and $\mathbf{B}(t)$ denote the state-transition matrix and process noise driven matrix, respectively, which can be obtained from (1) to (5) [3]. $(\cdot)_{m,n}$ means the first m rows and first n columns of the matrix $(\cdot)$.

Suppose that the installation error and scale factor error have been compensated, the velocity error induced by residual installation error and scale factor error can be modeled into the measurement noise. The difference between the velocity provided by DVL and SINS is utilized as the measurement, and the measurement model is formulated as

$$\mathbf{z}(t) = \mathbf{H}\mathbf{x}(t) + \boldsymbol{\eta}(t) = (\tilde{\mathbf{v}}^n)_{2,1} - (\tilde{\mathbf{v}}_{dvl}^n)_{2,1} \quad (8)$$

where $\mathbf{z}$ denotes the measurement vector, and $\boldsymbol{\eta}$ denotes the measurement noise. $\tilde{\mathbf{v}}^n = \mathbf{v}^n + \delta \mathbf{v}^n$ is the velocity provided by SINS, and $\mathbf{H} = \begin{bmatrix} -(\mathbf{v}^n \times)_{2,3} & \mathbf{I}_{2 \times 2} & \mathbf{0}_{2 \times 8} \end{bmatrix}$ denotes the measurement matrix.

Suppose that the sampling time is T_s, the discrete time index is k, and $t_k = kT_s$. Then, the discrete-time state-space model for SINS/DVL integrated navigation system can be obtained through equations (7) and (8)

$$\mathbf{x}_k = \mathbf{F}_k \mathbf{x}_{k-1} + \mathbf{G}_k \mathbf{w}_{k-1} \qquad (9)$$

$$\mathbf{z}_k = \mathbf{H}_k \mathbf{x}_k + \mathbf{v}_k \qquad (10)$$

where $\mathbf{x}_k = \mathbf{x}(t_k)$, $\mathbf{w}_k = \mathbf{w}(t_k)$, $\mathbf{z}_k = \mathbf{z}(t_k)$, $\mathbf{v}_k = \mathbf{v}(t_k)$, the state transition matrix $\mathbf{F}_k = \mathbf{I}_{13} + T_s \mathbf{A}(t_k)$, the process noise matrix is $\mathbf{G}_k = T_s \mathbf{B}(t_k)$, and the measurement matrix is $\mathbf{H}_k = \mathbf{H}$ [24].

Generally, the navigation errors of SINS/DVL integration can be estimated by Kalman filter through the state-space model (9)-(10), when the process noise and measurement noise are Gaussian distribution. However, in the case of severe manoeuvering, the output error of gyroscope will increase and be introduced into the SINS, which will increase the error of SINS. Thus, the statistic of the process noise changes into heavy-tailed distribution. Due to the complexity of underwater environment, the output of DVL may have outliers which will be introduced into measurement. As a result, the statistic of process noise and measurement noise go against the Gaussian assumption, which will degrade the performance of SINS/DVL integration based on the traditional KF. Aiming at this problem, a new robust Kalman filter for SINS/DVL integrated navigation system is proposed in this paper.

III. A NEW ROBUST SINS/DVL INTEGRATED NAVIGATION ALGORITHM

A. THE PROBABILITY DENSITY MODEL

For normal measurement, the measurement noise $\mathbf{v}_k$ can be described as a Gaussian distribution with zero mean vector and nominal covariance matrix $\mathbf{R}_k$. To address the outliers in measurement, a binary indicator variable λ_k modeled by beta-Bernoulli distribution is involved, which has been applied in outliers detection [19]–[21]. $\lambda_k = 0$ means that the measurement $\mathbf{z}_k$ is an outlier, while $\lambda_k = 1$ indicates $\mathbf{z}_k$ is a normal measurement. Thus, the measurement likelihood PDF $p(\mathbf{z}_k | \mathbf{x}_k, \lambda_k)$ can be formulated as

$$p(\mathbf{z}_k | \mathbf{x}_k, \lambda_k) = \mathrm{N}(\mathbf{z}_k; \mathbf{H}_k \mathbf{x}_k, \mathbf{R}_k)^{\lambda_k} \qquad (11)$$

where $\mathrm{N}(\mathbf{x}; \boldsymbol{\mu}, \boldsymbol{\Sigma})$ is the Gaussian PDF, $\boldsymbol{\mu}$ denotes mean vector $\mathbf{x}$, and $\boldsymbol{\Sigma}$ is covariance matrix of $\mathbf{x}$. Obviously, $\lambda_k = 1$ means that $p(\mathbf{z}_k | \mathbf{x}_k, \lambda_k)$ is a normal Gaussian distribution. For $\lambda_k = 0$, $p(\mathbf{z}_k | \mathbf{x}_k, \lambda_k)$ must be a constant, then, $\mathbf{z}_k$ is picked out and cannot be used for measurement update. Hence, the indicator variable λ_k is modelled by beta-Bernoulli hierarchical prior, and λ_k has a Bernoulli distribution controlled by beta variable π_k

$$p(\lambda_k | \pi_k) = \mathrm{Bn}(\lambda_k; \pi_k) = \pi_k{}^{\lambda_k}(1 - \pi_k)^{(1-\lambda_k)} \qquad (12)$$

where $\mathrm{Bn}(\cdot; \pi)$ denotes the Bernoulli PDF controlled by π, and π_k has a beta distribution controlled by parameters e_0 and f_0

$$p(\pi_k | e_0, f_0) = \mathrm{Be}(\pi_k; e_0, f_0) = \frac{\pi_k{}^{e_0-1}(1 - \pi_k)^{f_0-1}}{\mathrm{B}(e_0, f_0)} \qquad (13)$$

where $\mathrm{Be}(\cdot; e_0, f_0)$ denotes the beta PDF, and $\mathrm{B}(\cdot; \cdot)$ is beta function.

For heavy-tailed process noise, the one-step predicted PDF $p(\mathbf{x}_k | \mathbf{z}_{1:k-1})$ can be modelled as a Student's t-distribution as follow [16]

$$p(\mathbf{x}_k | \mathbf{z}_{1:k-1}) = \mathrm{St}(\mathbf{x}_k; \hat{\mathbf{x}}_{k|k-1}, \boldsymbol{\Sigma}_k, v_k) \qquad (14)$$

$\mathrm{St}(\cdot; \boldsymbol{\mu}, \boldsymbol{\Sigma}, v)$ is the Student's t PDF with mean vector $\boldsymbol{\mu}$, scale matrix $\boldsymbol{\Sigma}$, and dof parameter v. Since the Student's PDF can be regarded as mixed Gaussian PDFs, the equation (14) can be rewritten as [16]

$$\mathrm{St}(\mathbf{x}_k; \hat{\mathbf{x}}_{k|k-1}, \boldsymbol{\Sigma}_k, v_k) = \int_0^{+\infty} \mathrm{N}(\mathbf{x}_k; \hat{\mathbf{x}}_{k|k-1}, \frac{\boldsymbol{\Sigma}_k}{\xi_k}) \\ \times \mathrm{G}(\xi_k; \frac{v}{2}, \frac{v}{2}) d\xi_k \qquad (15)$$

where $\hat{\mathbf{x}}_{k|k-1}$ is predicted state with covariance matrix $\mathbf{P}_{k|k-1}$, ξ_k denotes an auxiliary random variable satisfied Gamma distribution, and $\mathrm{G}(\cdot; \alpha, \beta)$ is Gamma PDF with shape parameter α and rate parameter β. Employing equations (11)-(15), the likelihood PDF $p(\mathbf{z}_k | \mathbf{x}_k, \lambda_k)$ can be rewritten as follows

$$p(\mathbf{x}_k | \xi_k, \mathbf{z}_{1:k-1}) = \mathrm{N}(\mathbf{x}_k; \hat{\mathbf{x}}_{k|k-1}, \frac{\boldsymbol{\Sigma}_k}{\xi_k}) \qquad (16)$$

$$p(\xi_k) = \mathrm{G}(\xi_k; \frac{v}{2}, \frac{v}{2}) \qquad (17)$$

As the result that the inaccurate nominal process noise matrix $\mathbf{Q}_k$ has a great influence on the covariance matrix $\mathbf{P}_{k|k-1}$, $\mathbf{P}_{k|k-1}$ is not suitable to be utilized as scale matrix $\boldsymbol{\Sigma}_k$. Therefore, the scale matrix $\boldsymbol{\Sigma}_k$ is adaptively estimated by VB approach, and $\boldsymbol{\Sigma}_k$ is modelled as inverse Wishart distribution, i.e.,

$$p(\boldsymbol{\Sigma}_k) = \mathrm{IW}(\boldsymbol{\Sigma}_k; u_k, \mathbf{U}_k) \qquad (18)$$

where $\mathrm{IW}(\boldsymbol{\Sigma}_k; u_k, \mathbf{U}_k)$ is the inverse Wishart PDF, u_k is dof parameter of $\boldsymbol{\Sigma}_k$, and $\mathbf{U}_k$ is inverse scale matrix of $\boldsymbol{\Sigma}_k$. To obtain the prior information of scale matrix, the mean value of $p(\boldsymbol{\Sigma}_k)$ is set as

$$\frac{\mathbf{U}_k}{u_k - n - 1} = \mathbf{P}_{k|k-1} \qquad (19)$$

where

$$u_k = n + \tau + 1 \qquad (20)$$

$$\mathbf{U}_k = \tau \mathbf{P}_{k|k-1} \qquad (21)$$

where n is the dimension of $\mathbf{x}_k$, and $\tau \geq 0$ denotes a tuning parameter. Employing equations (11)-(13) and (16)-(18), a new robust SINS/DVL integrated navigation model is constructed.

B. THE THEORETICAL DERIVATION BASED ON VARIATIONAL BAYESIAN APPROACH

The next step is to jointly estimate the state vector, scale matrix, auxiliary random variable, Bernoulli variable, and beta variable through VB approach. Therefore, the jointly posterior PDF $p(\mathbf{\Theta}_k|\mathbf{z}_{1:k})$ needs to be calculated, where $\mathbf{\Theta}_k \triangleq \{\mathbf{x}_k, \boldsymbol{\xi}_k, \mathbf{\Sigma}_k, \lambda_k, \pi_k\}$. For hierarchical Gaussian state-space model, there is no analytical solution for $p(\mathbf{\Theta}_k|\mathbf{z}_{1:k})$. Thus, the VB method is adopted to obtain a free form factored approximate PDF for $p(\mathbf{\Theta}_k|\mathbf{z}_{1:k})$ to obtain an approximate solution, and $p(\mathbf{\Theta}_k|\mathbf{z}_{1:k})$ can be approximated as [25]

$$p(\mathbf{\Theta}_k|\mathbf{z}_{1:k}) \approx q(\mathbf{x}_k) q(\xi_k) q(\mathbf{\Sigma}_k) q(\lambda_k) q(\pi_k) \quad (22)$$

Suppose that ϕ is an arbitrary element of $\mathbf{\Theta}_k$, and $q(\phi)$ denotes the approximate PDF of ϕ. For standard VB approach, these approximate posterior PDFs in equation (22) subject to the equation as follow [16], [25]

$$\log q(\phi) = \mathrm{E}_{\mathbf{\Theta}_k^{(-\phi)}}[\log p(\mathbf{\Theta}_k, \mathbf{z}_{1:k})] + c_\phi \quad (23)$$

where $\mathbf{\Theta}_k^{-\phi}$ denotes all elements in $\mathbf{\Theta}_k$ except for ϕ, c_ϕ is the constant related to variable ϕ, and $\mathrm{E}[\cdot]$ is the expectation operation. For the fact that the variational parameters are coupled, the fixed-pointed iterations are used to obtain an approximate solution for (23) [3]. Thus, the $q(\phi)$ is updated as $q^{i+1}(\phi)$ at the $i + 1$th iteration.

Utilizing the conditional independence properties of the hierarchical state-space model, the joint PDF $p(\mathbf{\Theta}_k|\mathbf{z}_{1:k})$ can be factored as

$$p(\mathbf{\Theta}_k, \mathbf{z}_{1:k}) = p(\mathbf{z}_k|\mathbf{x}_k)p(\mathbf{x}_k|\xi_k, \mathbf{z}_{1:k-1})p(\xi_k)p(\mathbf{\Sigma}_k)$$
$$\times p(\lambda_k|\pi_k)p(\pi_k|e_0, f) p(\mathbf{z}_{1:k-1}) \quad (24)$$

Substituting (11)-(13) and (16)-(18) into (24) yields

$$p(\mathbf{\Theta}_k, \mathbf{z}_{1:k}) = \mathrm{N}(\mathbf{z}_k; \mathbf{H}_k\mathbf{x}_k, \mathbf{R}_k)^{\lambda_k} \mathrm{N}(\mathbf{x}_k; \hat{\mathbf{x}}_{k|k-1}, \frac{\mathbf{\Sigma}_k}{\xi_k})$$
$$\times \mathrm{G}(\xi_k; \frac{\nu}{2}, \frac{\nu}{2})\mathrm{IW}(\mathbf{\Sigma}_k; u_k, \mathbf{U}_k) \mathrm{Bn}(\lambda_k; \pi_k)$$
$$\times \mathrm{Be}(\pi_k; e_0, f_0) p(\mathbf{z}_{1:k-1}) \quad (25)$$

Taking the logarithm of both sides of equation (24) yields

$$\log p(\mathbf{\Theta}_k, \mathbf{z}_{1:k})$$
$$= -\frac{1}{2}\lambda_k (\mathbf{z}_k - \mathbf{H}_k x_k)^T \mathbf{R}_k^{-1} (\mathbf{z}_k - \mathbf{H}_k x_k)$$
$$- \frac{1}{2}\lambda_k \log |2\pi \mathbf{R}_k| - \frac{1}{2}\xi_k (\mathbf{x}_k - \hat{\mathbf{x}}_{k|k-1})^T \mathbf{\Sigma}_k^{-1} (\mathbf{x}_k - \hat{\mathbf{x}}_{k|k-1})$$
$$+ (\frac{n+\nu}{2} - 1) \log \xi_k - \frac{\nu \xi_k}{2} - \frac{1}{2}(n + u_k + 2) \log |\mathbf{\Sigma}_k|$$
$$- \frac{1}{2}\mathrm{tr}(\mathbf{U}_k \mathbf{\Sigma}_k^{-1}) + \lambda_k \log \pi_k + (1 - \lambda_k) \log (1 - \pi_k)$$
$$+ (e_0 - 1) \log \pi_k + (f_0 - 1) \log (1 - \pi_k) + c_{\mathbf{\Theta}_k} \quad (26)$$

Let $\phi = \lambda_k$ and utilizing (26) in (23) obtains

$$\log q^{(i+1)}(\lambda_k)$$
$$= -\frac{1}{2}\mathrm{E}_{\mathbf{\Theta}_k^{(-\lambda_k)}}^{(i)}[\lambda_k(\mathbf{z}_k - \mathbf{H}_k\mathbf{x}_k)^T \mathbf{R}_k^{-1} (\mathbf{z}_k \mathbf{H}_k - \mathbf{x}_k)]$$
$$- \frac{1}{2}\lambda_k \log |2\pi \mathbf{R}_k| + \lambda_k \mathrm{E}_{\mathbf{\Theta}_k^{(-\lambda_k)}}^{(i)} [\log \pi_k]$$
$$+ (1 - \lambda_k) \mathrm{E}_{\mathbf{\Theta}_k^{(-\lambda_k)}}^{(i)} [\log (1 - \pi_k)] + c_{\lambda_k}$$
$$= -\frac{1}{2}\lambda_k \mathrm{tr} \left[\mathbf{E}_k^{(i)} \mathbf{R}_k^{-1} \right] - \frac{1}{2}\lambda_k \log |2\pi \mathbf{R}_k|$$
$$+ \lambda_k \mathrm{E}_{\pi_k}^{(i)} [\log \pi_k] + (1 - \lambda_k) \mathrm{E}_{\pi_k}^{(i)} [\log (1 - \pi_k)] + c_{\lambda_k} \quad (27)$$

where

$$\mathbf{E}_k^{(i)} = \mathrm{E}_{\mathbf{\Theta}_k^{(-\lambda_k)}}^{(i)} \left[(\mathbf{z}_k - \mathbf{H}_k\mathbf{x}_k) (\mathbf{z}_k - \mathbf{H}_k\mathbf{x}_k)^T \right] \quad (28)$$

λ_k is a Bernoulli variable, thus

$$p^{(i+1)}(\lambda_k = 1) = A \exp \left\{ \mathrm{E}_{\pi_k}^{(i)}[\log \pi_k] - \frac{1}{2}\mathrm{tr}\{\mathbf{E}_k^{(i)} \mathbf{R}_k^{-1}\} \right.$$
$$\left. -\frac{1}{2} \log |2\pi \mathbf{R}_k| \right\} \quad (29)$$

$$p^{(i+1)}(\lambda_k = 0) = A \exp \left\{ \mathrm{E}_{\pi_k}^{(i)} [\log (1 - \pi_k)] \right\} \quad (30)$$

where the normalizing constant A is defined to make sure $p^{(i+1)}(\lambda_k = 1) + p^{(i+1)}(\lambda_k = 0) = 1$.

Let $\phi = \pi_k$ and substituting (26) into (23) yields

$$\log q^{(i+1)}(\pi_k)$$
$$= \mathrm{E}_{\mathbf{\Theta}_k^{(-\pi_k)}}^{(i+1)} [\lambda_k] \log \pi_k + (e_0 - 1) \log \pi_k$$
$$+ \{1 - \mathrm{E}_{\mathbf{\Theta}_k^{(-\pi_k)}}^{(i+1)}[\lambda_k]\} \log(1 - \pi_k)$$
$$+ (f_0 - 1) \log(1 - \pi_k) + c_{\pi_k}$$
$$= \{\mathrm{E}_{\lambda_k}^{(i+1)} [\lambda_k] + e_0 - 1\} \log \pi_k$$
$$+ \left\{ f_0 - \mathrm{E}_{\lambda_k}^{(i+1)} [\lambda_k] + 1 - 1 \right\}$$
$$\times \log (1 - \pi_k) + c_{\pi_k} \quad (31)$$

Employing (31), the approximated posterior PDF $q^{(i+1)}(\pi_k)$ can be updated as beta PDF controlled by parameter e_k and f_k, i.e.,

$$q^{(i+1)}(\pi_k) = \mathrm{Be}\left(\pi_k; e_k^{i+1}, f_k^{i+1}\right) \quad (32)$$

where

$$e_k^{i+1} = \mathrm{E}_{\lambda_k}^{(i+1)} [\lambda_k] + e_0 \quad (33)$$

$$f_k^{i+1} = f_0 - \mathrm{E}_{\lambda_k}^{(i+1)} [\lambda_k] + 1 \quad (34)$$

Let $\phi = \xi_k$ and using (26) in (23) obtains

$$\log q^{(i+1)}(\xi_k)$$
$$= -\frac{1}{2}\{E_{\Theta_k^{(-\xi_k)}}^{(i)}[(\mathbf{x}_k - \hat{\mathbf{x}}_{k|k-1})^T \boldsymbol{\Sigma}_k^{-1}(\mathbf{x}_k$$
$$- \hat{\mathbf{x}}_{k|k-1})] + \nu\}\xi_k + c_{\xi_k}$$
$$= (\frac{n+\nu}{2} - 1)\log \xi_k - \frac{1}{2}\left\{\mathrm{tr}\left[\mathbf{D}_k^{(i)}E_{\boldsymbol{\Sigma}_k}^{(i)}[\boldsymbol{\Sigma}_k^{-1}]\right] + \nu\right\}\xi_k$$
$$+ c_{\xi_k} \tag{35}$$

where

$$\mathbf{D}_k^{(i)} = E_{\mathbf{x}_k}^{(i)}\left[(\mathbf{x}_k - \hat{\mathbf{x}}_{k|k-1})(\mathbf{x}_k - \hat{\mathbf{x}}_{k|k-1})^T\right] \tag{36}$$

Using (35), the approximated posterior PDF $q^{(i+1)}(\xi_k)$ can be shown as a Gamma PDF as follow

$$q^{(i+1)}(\xi_k) = \mathrm{G}(\xi_k; \eta_k^{(i+1)}, \theta_k^{(i+1)}) \tag{37}$$

where

$$\eta_k^{(i+1)} = 0.5(n+\nu) \tag{38}$$
$$\theta_k^{(i+1)} = 0.5\left\{\nu + \mathrm{tr}\left[\mathbf{D}_k^{(i)}E_{\boldsymbol{\Sigma}_k}^{(i)}\left[\boldsymbol{\Sigma}_k^{-1}\right]\right]\right\} \tag{39}$$

Let $\phi = \boldsymbol{\Sigma}_k$ and substituting (26) into (23) yields

$$\log q^{i+1}(\boldsymbol{\Sigma}_k)$$
$$= -\frac{1}{2}E_{\Theta_k^{(-\Sigma_k)}}^{(i+1)}\left\{\xi_k(\mathbf{x}_k - \hat{\mathbf{x}}_{k|k-1})^T \boldsymbol{\Sigma}_k^{-1}(\mathbf{x}_k - \hat{\mathbf{x}}_{k|k-1})\right\}$$
$$- \frac{1}{2}(n + u_k + 2)\log|\boldsymbol{\Sigma}_k|$$
$$- \frac{1}{2}\mathrm{tr}(\mathbf{U}_k\boldsymbol{\Sigma}_k^{-1}) + c_{\Sigma_k}$$
$$= -\frac{1}{2}\mathrm{tr}\left\{\mathbf{U}_k\boldsymbol{\Sigma}_k^{-1} + E_{\xi_k}^{(i+1)}[\xi_k]\mathbf{D}_k^{(i)}\boldsymbol{\Sigma}_k^{-1}\right\}$$
$$- \frac{1}{2}(n + u_k + 2)\log|\boldsymbol{\Sigma}_k| + c_{\Sigma_k} \tag{40}$$

Employing (40), $q^{(i+1)}(\boldsymbol{\Sigma}_k)$ can be shown as

$$q^{(i+1)}(\boldsymbol{\Sigma}_k) = \mathrm{IW}(\boldsymbol{\Sigma}_k; \hat{u}_k^{(i+1)}, \hat{\mathbf{U}}_k^{(i+1)}) \tag{41}$$

where

$$\hat{u}_k^{(i+1)} = u_k + 1 \tag{42}$$
$$\hat{\mathbf{U}}_k^{(i+1)} = \mathbf{U}_k + E_{\xi_k}^{(i+1)}[\xi_k]\mathbf{D}_k^{(i)} \tag{43}$$

Let $\phi = \mathbf{x}_k$ and using (26) in (23) obtains

$$\log q^{(i+1)}(\mathbf{x}_k)$$
$$= -\frac{1}{2}E_{\Theta_k^{(-\mathbf{x}_k)}}^{(i+1)}[\lambda_k](\mathbf{z}_k - \mathbf{H}_k\mathbf{x}_k)^T\mathbf{R}_k^{-1}(\mathbf{z}_k$$
$$- \mathbf{H}_k\mathbf{x}_k) - \frac{1}{2}E_{\Theta_k^{(-\mathbf{x}_k)}}^{(i+1)}[\xi_k(\mathbf{x}_k - \hat{\mathbf{x}}_{k|k-1})^T\boldsymbol{\Sigma}_k^{-1}(\mathbf{x}_k - \hat{\mathbf{x}}_{k|k-1})]$$
$$+ c_{\mathbf{x}_k}$$
$$= -\frac{1}{2}E_{\lambda_k}^{(i+1)}[\lambda_k](\mathbf{z}_k - \mathbf{H}_k\mathbf{x}_k)^T\mathbf{R}_k^{-1}(\mathbf{z}_k - \mathbf{H}_k\mathbf{x}_k) + c_{\mathbf{x}_k}$$
$$- \frac{1}{2}E_{\xi_k}^{(i+1)}[\xi_k](\mathbf{x}_k - \hat{\mathbf{x}}_{k|k-1})^T E_{\boldsymbol{\Sigma}_k}^{(i+1)}\left[\boldsymbol{\Sigma}_k^{-1}\right](\mathbf{x}_k - \hat{\mathbf{x}}_{k|k-1})$$
$$= -\frac{1}{2}(\mathbf{z}_k - \mathbf{H}_k\mathbf{x}_k)^T\tilde{\mathbf{R}}_k^{-1}(\mathbf{z}_k - \mathbf{H}_k\mathbf{x}_k)$$
$$- \frac{1}{2}(\mathbf{x}_k - \hat{\mathbf{x}}_{k|k-1})^T\tilde{\mathbf{P}}_{k|k-1}^{-1}(\mathbf{x}_k - \hat{\mathbf{x}}_{k|k-1}) + c_{\mathbf{x}_k} \tag{44}$$

According to (44), the modified measurement noise matrix $\tilde{\mathbf{R}}_k^{(i+1)}$ and the modified predicted error covariance matrix $\tilde{\mathbf{P}}_{k|k-1}^{(i+1)}$ are given by

$$\tilde{\mathbf{R}}_k^{(i+1)} = \frac{\mathbf{R}_k}{E_{\lambda_k}^{(i+1)}[\lambda_k]} \tag{45}$$

$$\tilde{\mathbf{P}}_{k|k-1}^{(i+1)} = \frac{\left\{E_{\boldsymbol{\Sigma}_k}^{(i+1)}\left[\boldsymbol{\Sigma}_k^{-1}\right]\right\}^{-1}}{E_{\xi_k}^{(i+1)}[\xi_k]} \tag{46}$$

Using (44), $q^{(i+1)}(\mathbf{x}_k)$ can be updated as Gaussian PDF as follow

$$q^{(i+1)}(\mathbf{x}_k) = \mathrm{N}(\mathbf{x}_k; \hat{\mathbf{x}}_{k|k}^{(i+1)}, \mathbf{P}_{k|k}^{(i+1)}) \tag{47}$$

where mean vector $\hat{\mathbf{x}}_{k|k}^{(i+1)}$ and covariance matrix $\mathbf{P}_{k|k}^{(i+1)}$ can be updated by Kalman filter, i.e.,

$$\mathbf{K}_k^{(i+1)} = \tilde{\mathbf{P}}_{k|k-1}^{(i+1)}\mathbf{H}_k^T(\mathbf{H}_k\tilde{\mathbf{P}}_{k|k-1}^{(i)}\mathbf{H}_k^T + \tilde{\mathbf{R}}_k^{(i+1)})^{-1} \tag{48}$$
$$\hat{\mathbf{x}}_{k|k}^{(i+1)} = \hat{\mathbf{x}}_{k|k-1} + \mathbf{K}_k^{(i+1)}(\mathbf{z}_k - \mathbf{H}_k\hat{\mathbf{x}}_{k|k-1}) \tag{49}$$
$$\mathbf{P}_{k|k}^{(i+1)} = \left(\mathbf{I}_n - \mathbf{K}_k^{(i+1)}\mathbf{H}_k\right)\tilde{\mathbf{P}}_{k|k-1}^{(i+1)} \tag{50}$$

To mark the measurement outliers, we define λ_o as indicator value which is close to 0. When $E_{\lambda_k}^{(i+1)}[\lambda_k] \leq \lambda_o$, the measurement can be marked as an outlier which will be eliminated, and $q^{(i+1)}(\mathbf{x}_k)$ is updated by the predicted distribution, i.e.,

$$\hat{\mathbf{x}}_{k|k}^{(i+1)} = \hat{\mathbf{x}}_{k|k-1} \tag{51}$$
$$\mathbf{P}_{k|k}^{(i+1)} = \tilde{\mathbf{P}}_{k|k-1}^{(i+1)} \tag{52}$$

After N iterations, the approximate posterior PDFs in equation (22) can be updated as

$$q(x_k) \approx q^N(\mathbf{x}_k) = \mathrm{N}(\mathbf{x}_k; \hat{\mathbf{x}}_{k|k}^N, \mathbf{P}_{k|k}^N) \tag{53}$$
$$q(\xi_k) \approx q^N(\xi_k) = \mathrm{G}(\xi_k; \eta_k^N, \theta_k^N) \tag{54}$$
$$q(\boldsymbol{\Sigma}_k) \approx q^N(\boldsymbol{\Sigma}_k) = \mathrm{IW}(\boldsymbol{\Sigma}_k; \hat{u}_k^N, \hat{\mathbf{U}}_k^N) \tag{55}$$
$$q(\lambda_k) \approx q^N(\lambda_k) = \mathrm{Bn}\left(\lambda_k; p^N(\lambda_k = 1)\right) \tag{56}$$
$$q(\pi_k) \approx q^N(\pi_k) = \mathrm{Be}(\pi_k; e_k, f_k) \tag{57}$$

According to the property of each approximated posterior distribution, the required expectations are given by

$$E_{\xi_k}^{(i+1)}[\xi_k] = \frac{\eta_k^{i+1}}{\theta_k^{i+1}} \tag{58}$$

$$E_{\boldsymbol{\Sigma}_k}^{(i+1)}\left[\boldsymbol{\Sigma}_k^{-1}\right] = \left(\hat{u}_k^{i+1} - n - 1\right)\left(\hat{\mathbf{U}}_k^{i+1}\right)^{-1} \tag{59}$$

$$E_{\lambda_k}^{(i+1)}[\lambda_k] = \frac{p^{(i+1)}(\lambda_k = 1)}{p^{(i+1)}(\lambda_k = 1) + p^{(i+1)}(\lambda_k = 0)} \tag{60}$$

$$E_{\pi_k}^{(i+1)}[\log \pi_k] = \psi(e_k) - \psi(e_k + f_k + 1) \tag{61}$$
$$E_{\pi_k}^{(i+1)}[\log(1 - \pi_k)] = \psi(f_k + 1) - \psi(e_k + f_k + 1) \tag{62}$$

where $\psi(\cdot)$ is a digamma function. After updating (53), the required expectation $\mathbf{D}_k^{(i+1)}$ and $\mathbf{E}_k^{(i+1)}$ are calculated as

$$
\begin{aligned}
\mathbf{D}_k^{(i+1)} &= \mathrm{E}_{\mathbf{x}_k}^{(i+1)}\left[(\mathbf{x}_k - \hat{\mathbf{x}}_{k|k-1})(\mathbf{x}_k - \hat{\mathbf{x}}_{k|k-1})^T\right] \\
&= \mathrm{E}_{\mathbf{x}_k}^{(i+1)}\left[(\mathbf{x}_k - \hat{\mathbf{x}}_{k|k}^{i+1} + \hat{\mathbf{x}}_{k|k}^{i+1} - \hat{\mathbf{x}}_{k|k-1})\left(\mathbf{x}_k - \hat{\mathbf{x}}_{k|k}^{i+1}\right.\right. \\
&\quad \left.\left. + \hat{\mathbf{x}}_{k|k}^{i+1} - \hat{\mathbf{x}}_{k|k-1}\right)^T\right] \\
&= \mathrm{E}_{\mathbf{x}_k}^{(i+1)}\left[(\mathbf{x}_k - \hat{\mathbf{x}}_{k|k}^{i+1})(\mathbf{x}_k - \hat{\mathbf{x}}_{k|k}^{i+1})^T\right] \\
&\quad + (\hat{\mathbf{x}}_{k|k}^{i+1} - \hat{\mathbf{x}}_{k|k-1})\left(\hat{\mathbf{x}}_{k|k}^{i+1} - \hat{\mathbf{x}}_{k|k-1}\right)^T \\
&= \mathbf{P}_{k|k}^{(i+1)} + (\hat{\mathbf{x}}_{k|k}^{i+1} - \hat{\mathbf{x}}_{k|k-1})(\hat{\mathbf{x}}_{k|k}^{i+1} - \hat{\mathbf{x}}_{k|k-1})^T \quad (63)
\end{aligned}
$$

$$
\begin{aligned}
\mathbf{E}_k^{(i+1)} &= \mathrm{E}_{\boldsymbol{\Theta}_k^{(-\lambda_k)}}^{(i+1)}\left[(\mathbf{z}_k - \mathbf{H}_k\mathbf{x}_k)(\mathbf{z}_k - \mathbf{H}_k\mathbf{x}_k)^T\right] \\
&= \mathrm{E}_{\mathbf{x}_k}^{(i+1)}\left[\left(\mathbf{z}_k - \mathbf{H}_k\hat{\mathbf{x}}_{k|k}^{i+1} + \mathbf{H}_k\hat{\mathbf{x}}_{k|k}^{i+1} - \mathbf{H}_k x_k\right)\right. \\
&\quad \left.\left(\mathbf{z}_k - \mathbf{H}_k\hat{\mathbf{x}}_{k|k}^{i+1} + \mathbf{H}_k\hat{\mathbf{x}}_{k|k}^{i+1} - \mathbf{H}_k x_k\right)^T\right] \\
&= \left(\mathbf{z}_k - \mathbf{H}_k\hat{\mathbf{x}}_{k|k}^{i+1}\right)\left(\mathbf{z}_k - \mathbf{H}_k\hat{\mathbf{x}}_{k|k}^{i+1}\right)^T + \mathbf{H}_k\mathbf{P}_{k|k}^{i+1}\mathbf{H}_k^T \\
&\quad (64)
\end{aligned}
$$

The proposed robust Kalman filter for SINS/DVL integrated navigation system consists of (9), (10), (18)-(21), (32)-(34), (37-39), (41)-(43), (45)-(52), and (58)-(64), and the implementation pseudo-code for the proposed algorithm is shown in Algorithm 1. For the process uncertainty, we obtained a modified one-step predicted covariance matrix to suppress the influence of process uncertainty. For the measurement noise, we use an indicator variable to detect the useless outliers and remove it, and we also obtained a modified measurement noise covariance matrix to adapt the variation of measurement noise. The corresponding block diagram of the proposed SINS/DVL integrated navigation method is shown in Fig. 1. The proposed robust Kalman filter is adopted to estimate the navigation errors, and the navigation errors can correct the navigation parameters with output correction method.

IV. TEST RESULT
In order to verify the validity of the proposed robust Kalman filter, a sea trial experiment is carried out to verify the performance of SINS/DVL integrated navigation algorithm based on the proposed filter. The experimental equipments consist of the photonics inertial navigation system (PHINS), self-made fiber-optic-SINS (FSINS), Doppler velocity log, and global position system (GPS) receiver. The specific force $\mathbf{f}^b$ and rotation rate $\boldsymbol{\omega}_{ib}^b$ are provided by the FSINS equipped with accelerometers (bias 10^{-4}g, noise 10^{-5}g$/\sqrt{\text{Hz}}$) and gyroscopes (drift $0.01°$/h, noise $0.1°$/h$/\sqrt{\text{Hz}}$), and the ground velocity is provided by DVL (noise: standard variance 0.3m/s). The outputs attitude, velocity, and position of GPS/PHINS high-accuracy integration navigation system are used as the reference, the accuracy of reference attitude is $0.01°$, the accuracy of reference velocity is 0.1m/s, and

---

Algorithm 1 One Time Step of the Proposed KF

Inputs: $\hat{\mathbf{x}}_{k-1|k-1}$, $\mathbf{P}_{k-1|k-1}$, $\mathbf{F}_k$, $\mathbf{G}_k$, $\mathbf{H}_k$, $\mathbf{z}_k$, $\mathbf{Q}_{k-1}$, $\mathbf{R}_k$, e_0, f_0, ν, τ, n, N, λ_o.
Time update:
1. Update $\hat{\mathbf{x}}_{k|k-1}$ and $\mathbf{P}_{k|k-1}$.
$\hat{\mathbf{x}}_{k|k-1} = \mathbf{F}_k\hat{\mathbf{x}}_{k-1|k-1}$
$\mathbf{P}_{k|k-1} = \mathbf{F}_k\mathbf{P}_{k-1|k-1}\mathbf{F}_k^T + \mathbf{G}_k\mathbf{Q}_{k-1}\mathbf{G}_k^T$
Measurement update:
2. Initialization: $u_k = n + \tau + 1$, $\mathbf{U}_k = \tau\mathbf{P}_{k|k-1}$, $e_k^0 = e_0$, $f_k^0 = f_0$, $\mathrm{E}_{\Sigma_k}^{(0)}\left[\boldsymbol{\Sigma}_k^{-1}\right] = (u_k - n - 1)\mathbf{U}_k^{-1}$, $\hat{\mathbf{x}}_{k|k}^{(0)} = \hat{\mathbf{x}}_{k|k-1}$ and $\mathbf{P}_{k|k}^{(0)} = \mathbf{P}_{k|k-1}$.
for $i = 0 : N - 1$
3. Update $q^{(i+1)}(\lambda_k) = \text{Bn}\left(\lambda_k; p^{(i+1)}(\lambda_k = 1)\right)$
$\mathbf{E}_k^{(i)} = \left(\mathbf{z}_k - \mathbf{H}_k\hat{\mathbf{x}}_{k|k}^{(i)}\right)\left(\mathbf{z}_k - \mathbf{H}_k\hat{\mathbf{x}}_{k|k}^{(i)}\right)^T + \mathbf{H}_k\mathbf{P}_{k|k}^{(i)}\mathbf{H}_k^T$
$\mathrm{E}_{\pi_k}^{(i+1)}\left[\log\pi_k\right] = \psi\left(e_k^i\right) - \psi\left(e_k^i + f_k^i\right)$
$\mathrm{E}_{\pi_k}^{(i+1)}\left[\log(1 - \pi_k)\right] = \psi\left(f_k^i\right) - \psi\left(e_k^i + f_k^i\right)$
$p^{(i+1)}(\lambda_k = 1) = A\exp\left\{\mathrm{E}_{\pi_k}^{(i+1)}\left[\log\pi_k\right] - 0.5\text{tr}\left\{\mathbf{E}_k^{(i)}\mathbf{R}_k^{-1}\right\}\right.$
$\left. -0.5\log|2\pi\mathbf{R}_k|\right\}$
$p^{(i+1)}(\lambda_k = 0) = A\exp\left\{\mathrm{E}_{\pi_k}^{(i+1)}\left[\log(1 - \pi_k)\right]\right\}$
$\mathrm{E}_{\lambda_k}^{(i+1)}[\lambda_k] = p^{(i+1)}(\lambda_k = 1)/\left(p^{(i+1)}(\lambda_k = 1) + p^{(i+1)}(\lambda_k = 0)\right)$
4. Update $q^{(i+1)}(\pi_k) = \text{Be}\left(\pi_k; e_k^{i+1}, f_k^{i+1}\right)$
$e_k^{i+1} = \mathrm{E}_{\lambda_k}^{(i+1)}[\lambda_k] + e_0$, $f_k^{i+1} = f_0 - \mathrm{E}_{\lambda_k}^{(i+1)}[\lambda_k] + 1$
5. Update $q^{(i+1)}(\xi_k) = \text{G}(\xi_k; \eta_k^{(i+1)}, \theta_k^{(i+1)})$
$\mathbf{D}_k^{(i)} = \mathbf{P}_{k|k}^{(i)} + (\hat{\mathbf{x}}_{k|k}^i - \hat{\mathbf{x}}_{k|k-1})(\hat{\mathbf{x}}_{k|k}^i - \hat{\mathbf{x}}_{k|k-1})^T$,
$\eta_k^{(i+1)} = 0.5(n + \nu)$
$\theta_k^{(i+1)} = 0.5\left\{\nu + \text{tr}\left[\mathbf{D}_k^{(i)}\mathrm{E}_{|bm\Sigma_k}^{(i)}\left[\boldsymbol{\Sigma}_k^{-1}\right]\right]\right\}$,
$\mathrm{E}_{\xi_k}^{(i+1)}[\xi_k] = \eta_k^{i+1}/\theta_k^{i+1}$
6. Update $q^{(i+1)}(\boldsymbol{\Sigma}_k) = \text{IW}(\boldsymbol{\Sigma}_k; \hat{u}_k^{(i+1)}, \hat{\mathbf{U}}_k^{(i+1)})$
$\hat{u}_k^{(i+1)} = u_k + 1$, $\hat{\mathbf{U}}_k^{(i+1)} = \mathbf{U}_k + \mathrm{E}_{\xi_k}^{(i+1)}[\xi_k]\mathbf{D}_k^{(i)}$,
$\mathrm{E}_{\Sigma_k}^{(i+1)}\left[\boldsymbol{\Sigma}_k^{-1}\right] = \left(\hat{u}_k^{i+1} - n - 1\right)\left(\hat{\mathbf{U}}_k^{i+1}\right)^{-1}$
7. Update $q^{(i+1)}(\mathbf{x}_k) = \text{N}(\mathbf{x}_k; \hat{\mathbf{x}}_{k|k}^{(i+1)}, \mathbf{P}_{k|k}^{(i+1)})$
$\tilde{\mathbf{R}}_k^{i+1} = \mathbf{R}_k/\mathrm{E}_{\lambda_k}^{(i+1)}[\lambda_k]$,
$\tilde{\mathbf{P}}_{k|k-1}^{(i+1)} = \left\{\mathrm{E}_{\mathbf{P}_{k|k-1}}^{(i+1)}\left[\mathbf{P}_{k|k-1}^{-1}\right]\right\}^{-1}/\mathrm{E}_{\xi_k}^{(i+1)}[\xi_k]$,
$\mathbf{K}_k^{(i+1)} = \tilde{\mathbf{P}}_{k|k-1}^{(i+1)}\mathbf{H}_k^T(\mathbf{H}_k\tilde{\mathbf{P}}_{k|k-1}^{(i+1)}\mathbf{H}_k^T + \tilde{\mathbf{R}}_k)^{-1}$,
$\hat{\mathbf{x}}_{k|k}^{(i+1)} = \hat{\mathbf{x}}_{k|k-1} + \mathbf{K}_k^{(i+1)}(\mathbf{z}_k - \mathbf{H}_k\hat{\mathbf{x}}_{k|k-1})$,
$\mathbf{P}_{k|k}^{(i+1)} = \left(\mathbf{I}_n - \mathbf{K}_k^{(i+1)}\mathbf{H}_k\right)\tilde{\mathbf{P}}_{k|k-1}^{(i+1)}$
if $\mathrm{E}_{\lambda_k}^{(i+1)}[\lambda_k] \leq \lambda_o$
$\hat{\mathbf{x}}_{k|k}^{(N)} = \hat{\mathbf{x}}_{k|k-1}$, $\mathbf{P}_{k|k}^{(N)} = \tilde{\mathbf{P}}_{k|k-1}^{(i+1)}$, $i = N$
end
end for
8. $\hat{\mathbf{x}}_{k|k} = \hat{\mathbf{x}}_{k|k}^{(N)}$, $\mathbf{P}_{k|k} = \mathbf{P}_{k|k}^{(N)}$
Outputs: $\hat{\mathbf{x}}_{k|k}$ and $\mathbf{P}_{k|k}$

---

the accuracy of reference position is $5 - 20$m. The total test time is 5400s, and the trajectory, heading angle, and heading rate provided by the reference are shown in Fig. 2-Fig. 3.
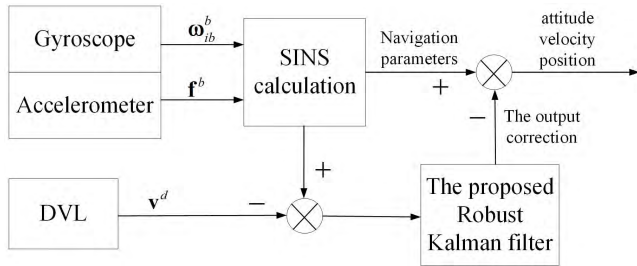
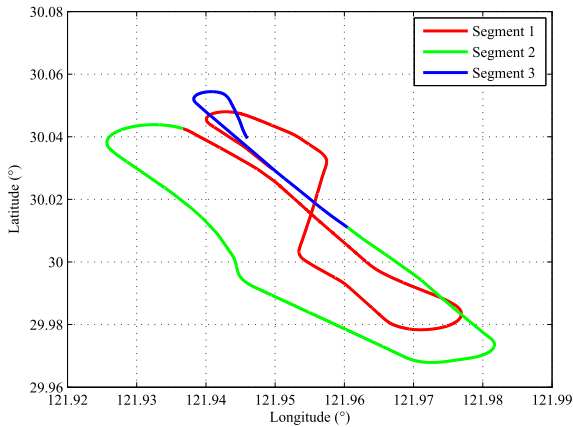**FIGURE 1.** The block diagram of SINS/DVL integrated navigation method.

FIGURE 2. The trajectory of the ship.

FIGURE 3. The heading angle and heading rate of the ship.

FIGURE 4. The PDF of the DVL measurement noise.

As shown in Fig. 2-Fig. 3, the ship maneuvered severely with several turns before the former 4000s and sailed smoothly from 4000s to 5400s, thus the process uncertainty is induced by severe manoeuvering [3]. The measurement noise can be calculated by the reference velocity and the velocity provided by DVL, and the PDF of the measurement noises are plotted in Fig. 4. The enlarged portion in Fig. 4 shows that the velocity provided by DVL contains some outliers, and the RMS error of the velocity with outliers is 1.2 m/s. Therefore, the experiment data can be used to verify the performance of the proposed KF.
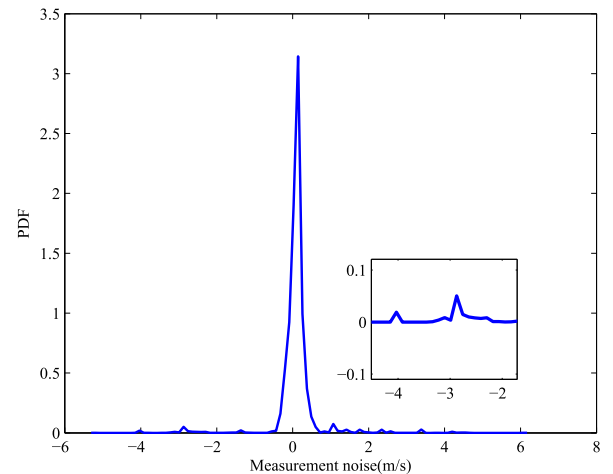
In this paper, we carried out three tests with different data segments which has been plotted in Fig. 2, and each data segment lasts 1800s. To verify the performance of the proposed algorithm, the proposed KF is tested by the three data segments and compared with existing KF,

TABLE 1. The RMSs of the attitude errors of different filtering algorithms.

Attitude errors	Segment	KF	RSTKF	ODKF	ISODKF	The proposed KF
	Segment 1	0.09	0.08	0.08	0.08	0.08
Pitch error (°)	Segment 2	0.09	0.06	0.06	0.06	0.06
	Segment 3	0.05	0.05	0.05	0.05	0.03
	Segment 1	0.02	0.02	0.02	0.02	0.02
Roll error (°)	Segment 2	0.06	0.03	0.03	0.03	0.02
	Segment 3	0.02	0.02	0.02	0.02	0.02
	Segment 1	0.86	0.17	0.43	0.42	0.14
Heading error (°)	Segment 2	0.79	0.17	0.32	0.32	0.12
	Segment 3	0.42	0.11	0.35	0.35	0.07

TABLE 2. The RMSs of the velocity errors of different filtering algorithms.

Velocity errors	Segment	KF	RSTKF	ODKF	ISODKF	The proposed KF
East velocity error (m/s)	Segment 1	0.38	0.23	0.22	0.22	0.14
	Segment 2	0.45	0.34	0.33	0.33	0.20
	Segment 3	0.28	0.22	0.19	0.19	0.15
North velocity error (m/s)	Segment 1	0.51	0.22	0.26	0.26	0.16
	Segment 2	0.55	0.19	0.17	0.17	0.12
	Segment 3	0.27	0.21	0.17	0.17	0.12

TABLE 3. The RMSs of the position errors of different filtering algorithms.

Position errors	Segment	KF	RSTKF	ODKF	ISODKF	The proposed KF
Latitude error (°)	Segment 1	0.0025	0.0007	0.0019	0.0019	0.0003
	Segment 2	0.0026	0.0006	0.0019	0.0019	0.0002
	Segment 3	0.0025	0.0009	0.0015	0.00015	0.0002
Longitude error (°)	Segment 1	0.0018	0.0012	0.0016	0.0016	0.0011
	Segment 2	0.0010	0.0008	0.0009	0.0009	0.0006
	Segment 3	0.0021	0.0011	0.0015	0.0015	0.0009

TABLE 4. The implementation times in a single step run of different filtering algorithms.

Algorithms	Time (s)
KF	4.30×10^{-5}
RSTKF	3.42×10^{-4}
ODKF	2.08×10^{-4}
ISODKF	6.15×10^{-5}
The proposed KF	7.64×10^{-4}

FIGURE 5. The attitude angle errors from different algorithms.

RSTKF [16], ODKF [19], and outlier detection KF based on innovation standard deviation (ISODKF) [26]. The corresponding parameters are set as follow: the initial state is $x_{0|0} = 0_{13 \times 1}$, and the state error covariance matrix is $\mathbf{P}_{0|0} = \text{diag}([0.1°; 0.1°; 0.1°; 0.1\text{m/s}; 0.1\text{m/s}; 1°/\text{h}; 1°/\text{h}; 0.01°/\text{h}; 0.01°/\text{h}; 0.01°/\text{h}; 10^{-4}g; 10^{-4}g; 10^{-4}g])^2$. The nominal process noise and measurement noise covariance matrixes are set as $\mathbf{Q}_k = \text{diag}([0.01°/\text{h}; 0.01°/\text{h}; 0.01°/\text{h}; 2.5 \times 10^{-3}g; 2.5 \times 10^{-3}g; 2.5 \times 10^{-3}g])^2$ and $\mathbf{R}_k = \text{diag}([0.3\text{m/s}; 0.3\text{m/s}])^2$ respectively. The tuning parameter is $\tau = 5$, and the dof parameter is $\nu = 5$ [16]. For the proposed KF, the parameters are chosen as $e_0 = 0.9$, $f_0 = 0.1$, and the iteration numbers of all robust filters are all set as $N = 3$ [19]. The indicator value is selected as $\lambda_o = 1 \times 10^{-10}$ [19] to detect the measurement outliers effectively. The corresponding root mean square (RMSs) of the attitude error, velocity error, and position error of
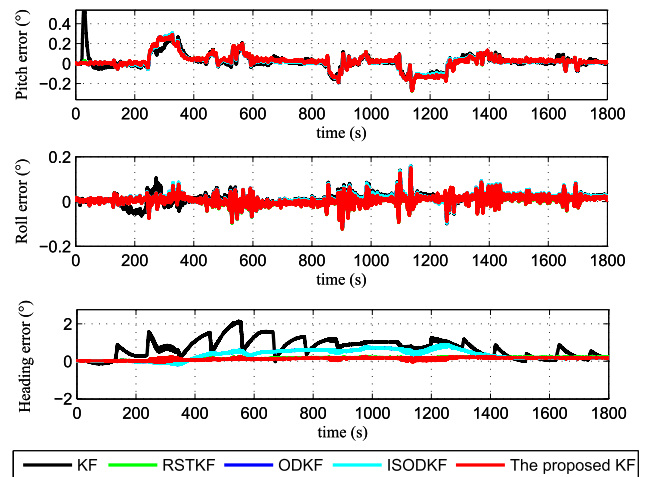
the three tests are summarized in Table 1-Table 3, and the implementation times in a single step run of different filtering algorithms are summarized in Table 4. To show the single run results, the attitude errors, velocity errors, and position errors of the SINS/DVL integrated navigation system of the segment 1 are plotted in Fig. 5-Fig. 7.

As shown in Fig. 5-Fig. 7 and Table 1-Table 3, the pitch error and the roll error calculated by the existing KF, RSTKF, ODKF, ISODKF and the proposed KF are almost the same, but the heading error calculated by the KF is bigger than the other four algorithms. Besides, the velocity errors and position errors calculated by the proposed KF are smaller than that calculated by the KF, ODKF, ISODKF,
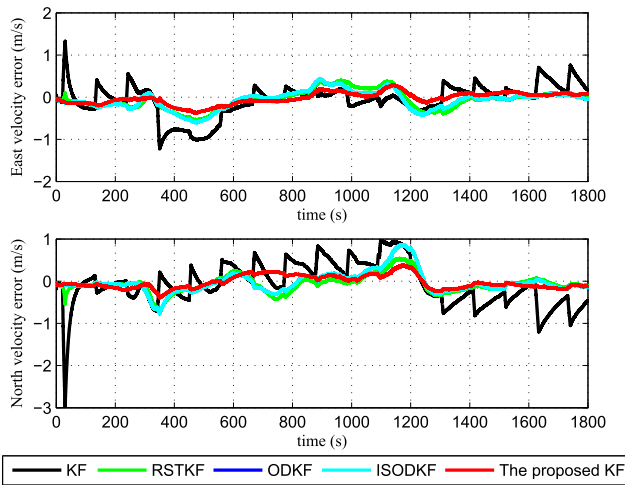
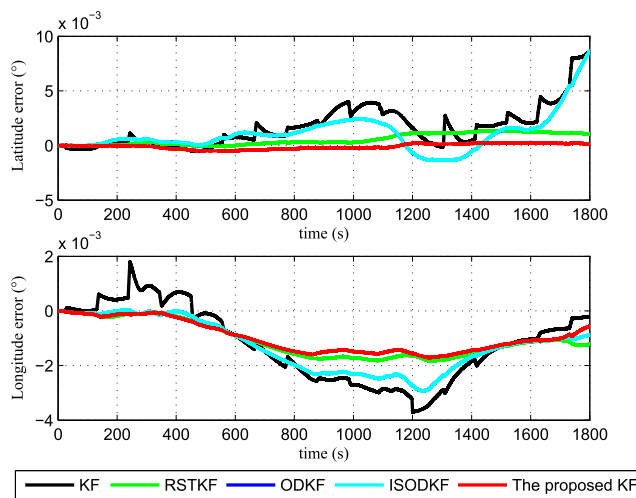**FIGURE 6.** The velocity errors from different algorithms.

FIGURE 7. The position errors from different algorithms.

and RSTKF. Table 4 shows that the computational times of all algorithms are far less than the sampling period 0.01s, which can meet the requirement of SINS/DVL integrated navigation system. Note that due to the influence of the heavy-tailed distribution process noise induced by process uncertainty, the process noise is violated with Gaussian distribution, which will degrade the performance of the ODKF and ISODKF. For RSTKF, useless measurement outliers are also introduced in the filter, which will result in performance degradation of the RSTKF. The proposed KF address the process uncertainty and measurement outliers by modelling the one-step predicted as a Student's t-distribution and the binary indicator variable as beta-Bernoulli distribution, and the useless measurement outliers can be accurately eliminated, thus the proposed KF exhibit better robustness and higher accuracy. In a word, compared with the existing state-of-the-art algorithms, the proposed KF for SINS/DVL integrated navigation system has better robustness and navigation accuracy to address process uncertainty and measurement outliers.

V. CONCLUSION

To suppress the process uncertainty and measurement outlier of SINS/DVL integrated navigation system, a novel robust KF is proposed in this paper. By modelling the one-step predicted as Student's t-distribution and the binary indicator variable as beta-Bernoulli distribution, the proposed KF for SINS/DVL integrated navigation system is able to suppress the process uncertainty and measurement outliers induced by severe maneuvering and obtain better navigation accuracy than the other four algorithms. Experimental results illustrate that the proposed algorithm has better robustness and navigation accuracy for suppression of the process uncertainty and measurement outliers than the state-of-the-art SINS/DVL integrated navigation algorithms, which is more suitable for SINS/DVL integrated navigation system.

REFERENCES

[1] Y. Tang, Y. Wu, M. Wu, W. Wu, X. Hu, and L. Shen, "INS/GPS integration: Global observability analysis," *IEEE Trans. Veh. Technol.*, vol. 58, no. 3, pp. 1129–1142, Mar. 2009.

[2] Y. Zhang, L. Luo, T. Fang, N. Li, and G. Wang, "An improved coarse alignment algorithm for odometer-aided sins based on the optimization design method," *Sensors*, vol. 18, no. 1, p. 195, Jan. 2018.

[3] Y. Huang and Y. Zhang, "A new process uncertainty robust student's t based Kalman filter for SINS/GPS integration," *IEEE Access*, vol. 5, pp. 14391–14404, 2017.

[4] W. Gao, J. Li, G. Zhou, and Q. Li, "Adaptive Kalman filtering with recursive noise estimator for integrated SINS/DVL systems," *J. Navigat.*, vol. 68, no. 1, pp. 142–161, Jan. 2015.

[5] Y. Zhang, "An approach of DVL-aided SDINS alignment for in-motion vessel," *Optik*, vol. 124, no. 23, pp. 6270–6275, Dec. 2013.

[6] Y. Huang, Y. Zhang, Z. Wu, N. Li, and J. Chambers, "A novel adaptive Kalman filter with inaccurate process and measurement noise covariance matrices," *IEEE Trans. Autom. Control*, vol. 63, no. 2, pp. 594–601, Feb. 2018.

[7] L. Chang, K. Li, and B. Hu, "Huber's M-estimation-based process uncertainty robust filter for integrated INS/GPS," *IEEE Sensors J.*, vol. 15, no. 6, pp. 3367–3374, Jun. 2015.

[8] M. C. Graham, J. P. How, and D. E. Gustafson, "Robust state estimation with sparse outliers," *J. Guid. Control Dyn.*, vol. 38, no. 7, pp. 1229–1240, 2015.

[9] X. R. Li and Y. Bar-Shalom, "A recursive multiple model approach to noise identification," *IEEE Trans. Aerosp. Electron. Syst.*, vol. 30, no. 3, pp. 671–684, Jul. 1994.

[10] H. Qian, D. An, and Q. Xia, "IMM-UKF based land-vehicle navigation with low-cost GPS/INS," in *Proc. IEEE Int. Conf. Inf. Autom.*, Jun. 2010, pp. 2031–2035.

[11] X. Gao, D. You, and S. Katayama, "Seam tracking monitoring based on adaptive Kalman filter embedded elman neural network during high-power fiber laser welding," *IEEE Trans. Ind. Electron.*, vol. 59, no. 11, pp. 4315–4325, Nov. 2012.

[12] S. Sarkka and A. Nummenmaa, "Recursive noise adaptive Kalman filtering by variational Bayesian approximations," *IEEE Trans. Autom. Control*, vol. 54, no. 3, pp. 596–600, Mar. 2009.

[13] R. K. Mehra, "Approaches to adaptive filtering," *IEEE Trans. Autom. Control*, vol. 17, no. 5, pp. 693–698, Oct. 1972.

[14] Y. Huang, Y. Zhang, N. Li, and J. Chambers, "Robust student's t based nonlinear filter and smoother," *IEEE Trans. Aerosp. Electron. Syst.*, vol. 52, no. 5, pp. 2586–2596, Oct. 2017.

[15] M. Roth and E. Özkan, and F. Gustafsson, "A student's t filter for heavy tailed process and measurement noise," in *Proc. IEEE Int. Conf. Acoust. Speech Signal Process.*, May 2013, pp. 5770–5774.

[16] Y. Huang, Y. Zhang, Z. Wu, N. Li, and J. A. Chambers, "A novel robust student's t-based Kalman filter," *IEEE Trans. Aerosp. Electron. Syst.*, vol. 53, no. 3, pp. 1545–1554, Jun. 2017.

[17] Y. Huang, Y. Zhang, P. Shi, Z. Wu, J. Qian, and J. A. Chambers, ''Robust Kalman filters based on Gaussian scale mixture distributions with application to target tracking,'' *IEEE Trans. Syst. Man, Cybern., Syst.*, to be published.

[18] Y. Huang, Y. Zhang, B. Xu, Z. Wu, and J. Chambers, ''A new outlier-robust student's t based Gaussian approximate filter for cooperative localization,'' *IEEE-ASME Trans. Mechatronics*, vol. 22, no. 5, pp. 2380–2386, Oct. 2017.

[19] H. Wang, H. Li, J. Fang, and H. Wang, ''Robust Gaussian Kalman filter with outlier detection,'' *IEEE Signal Process. Lett.*, vol. 25, no. 8, pp. 1236–1240, Aug. 2018.

[20] Q. Wan, H. Duan, J. Fang, H. Li, and Z. Xing, ''Robust Bayesian compressed sensing with outliers,'' *Signal Process.*, vol. 140, pp. 104–109, Nov. 2017.

[21] X. Ding, L. He, and L. Carin, ''Bayesian robust principal component analysis,'' *IEEE Trans. Image Process.*, vol. 20, no. 12, pp. 3419–3430, Dec. 2011.

[22] D. Titterton and J. Weston, *Strapdown Inertial Navigation Technology*, 2nd ed. London, U.K.: Lavenham Press, 2004.

[23] G. D. Paul, *Principles of GNSS, Inertial, and Multisensor Integrated Navigation Systems*, 2nd ed. Norwood, MA, USA: Artech House, 2013.

[24] D. Simon, *Optimal State Estimation: Kalman, H8, and Nonlinear Approaches*. Hoboken, NJ, USA: Wiley, 2006.

[25] D. G. Tzikas, C. L. Likas, and N. P. Galatsanos, ''The variational approximation for Bayesian inference,'' *IEEE Signal Process. Mag.*, vol. 25, no. 6, pp. 131–146, Nov. 2008.

[26] Z. M. Zhu, H. X. Qiu, J.-S. Li, and Y. X. Huang, ''Identification and elimination of outliers in dynamic measurement data,'' *Syst. Eng. Electron.*, vol. 26, no. 2, pp. 147–149, Feb. 2004.
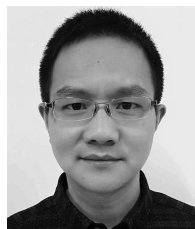
YONGGANG ZHANG received the B.S. and M.S. degrees from the Department of Automation, Harbin Engineering University (HEU), Harbin, China, in 2002 and 2004, respectively, and the Ph.D. degree in electronic engineering from Cardiff University, U.K., in 2007. He was a Post-doctoral Fellow in adaptive signal processing with Loughborough University, U.K., from 2007 to 2008. He is currently a Professor of navigation, guidance, and control with HEU. His current research interests include signal processing, information fusion, and their applications in navigation technology, such as fiber optical gyroscope, inertial navigation, and integrated navigation.

TAO FANG received the B.S. degree from the School of Electrical and Control Engineering, North University of China, Taiyuan, China, in 2014. He is currently pursuing the Ph.D. degree in control science and engineering with the College of Automation, Harbin Engineering University, Harbin, China. Since 2018, he has been a Visiting Graduate Researcher with the Department of Electrical and Computer Engineering, University of Alberta, Edmonton, AB, Canada. His current research interests include polar navigation, and information fusion and its application in integrated navigation systems.
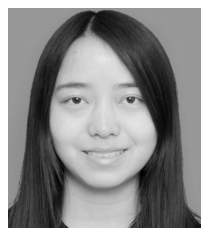
LI LUO received the B.S. and M.S. degrees from the College of Automation, Harbin Engineering University, Harbin, China, in 2015 and 2017, respectively, where she is currently pursuing the Ph.D. degree in control science and engineering. Her current research interest includes information fusion and its application in integrated navigation systems.

NING LI received the bachelor's, master's, and Ph.D. degrees from the College of Automation, Harbin Engineering University, Harbin, China, in 2002, 2005, and 2009, respectively. She was an Academic Visitor with Cardiff University, from 2006 to 2007, and also with the University of Surrey, from 2017 to 2018. She is currently an Associate Professor of control science and engineering with Harbin Engineering University. Her research interests include integrated navigation and adaptive filtering methods.

• • •